

Novel nano molten salt tetra-2,3-pyridiniumporphyrizinato-oxo-vanadium tricyanomethanide as a vanadium surface free phthalocyanine catalyst: application to the Strecker synthesis of α -aminonitrile derivatives

Saeed Bagheri,^a Mohammad Ali Zolfigol,^{*a} Maliheh Safaiee,^b Diego A. Alonso,^{*c} Abbas Khoshnood^{*c}

^a*Department of Organic Chemistry, Faculty of Chemistry, Bu-Ali Sina University, Hamedan 6517838683, Iran.*

^b*Department of Medicinal Plants Production, Nahavand University, Nahavand, 6593139565, Iran.*

^c*Instituto de Síntesis Orgánica and Departamento de Química Orgánica, Universidad de Alicante, Apdo. 99, 03080 Alicante, Spain.*

**Corresponding Author: Fax:^a +988138380709. *Corresponding Author: Phone:^c +34965909841*

E-mail: zolfi@basu.ac.ir, mzolfigol@yahoo.com (M.A. Zolfigol), diego.alonso@ua.es (Diego A. Alonso); abbas.khoshnood@ua.es (Abbas Khoshnood)

Abstract: An efficient and recyclable novel nano tetra-2,3-pyridiniumporphyrinato-oxo-vanadium tricyanomethanide $\{[\text{VO}(\text{TPPA})][\text{C}(\text{CN})_3]_4\}$ as a vanadium surface free phthalocyanine based molten salt catalyst was successfully designed, produced, and used for the Strecker synthesis of α -aminonitrile derivatives through a one-pot three-component reaction between aromatic aldehydes, trimethylsilyl cyanide (TMSCN), and aniline derivatives under neat conditions at 50 °C. This catalyst was well characterized by Fourier transform infrared spectroscopy (FT-IR), UV-visible spectroscopy (UV-Vis), X-ray diffraction (XRD), X-ray photoelectron spectroscopy (XPS), scanning electron microscopy (SEM), high resolution transmission electron microscopy (HRTEM), energy-dispersive X-ray spectroscopy (EDX), inductive coupling plasma mass spectrometer (ICP-MS), and thermal gravimetric (TGA) analysis. The catalyst can be simply recovered and reused several times without significant loss of catalytic activity.

Keywords: Nano tetra-2,3-pyridiniumporphyrinato-oxo-vanadium tricyanomethanide, Phthalocyanine, molten salt, Strecker synthesis, α -aminonitrile, neat conditions.

1. Introduction

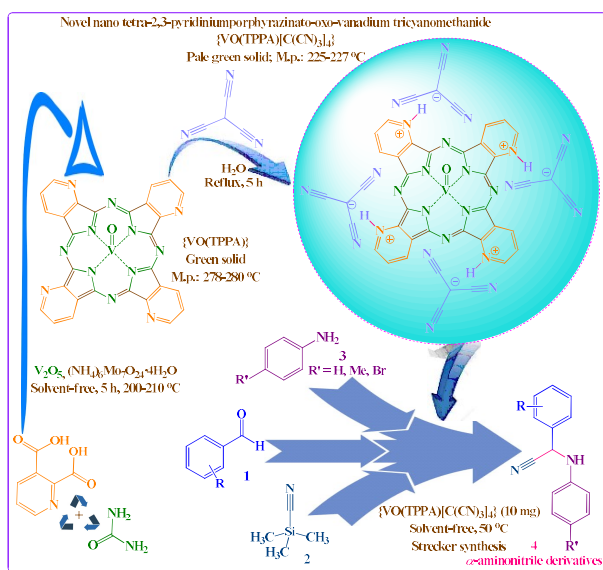
Metal phthalocyanines (MPcs) are stable and simply attainable macro cyclic complexes employed as cost-effective biomimetic oxidation catalysts and with numerous applications in organic synthesis.¹⁻⁷ Phthalocyanine derivatives are usually produced *via* high-temperature cyclotetramerization of phthalic acid or dicyano derivatives.⁸⁻¹⁶ Metal ion templates can significantly increase the yields of these reactions.^{8,10,12-14} Heterocyclic phthalocyanine derivatives containing pyridine, thionaphthalene, thiophene, and pyrazine rings¹⁷ have been also synthesized and deeply studied. Metal complexes of tetrapyrrolineporphyrins (pyridine derivatives),¹⁸ are prepared using a template process similar to that of phthalocyanine.¹⁹⁻²² Moreover, various syntheses of metallo-tetrapyrrolineporphyrins by 2,3- and 3,4-pyridinedicarboxylic acid have been also reported.²³⁻²⁹

The Strecker synthesis, firstly reported in 1850,^{30a} is the oldest known multi component reaction and the most facile method for the synthesis of α -amino acids on both lab and technical scales. The Strecker reaction includes a condensation of an aldehyde with ammonia, in the presence of a cyanide source to form α -aminonitriles, which are subsequently hydrolyzed to the corresponding amino acids.³⁰ α -Aminonitriles are popular bifunctional synthons that have found numerous synthetic uses, being the synthesis of amino acids the most important one.³¹ Both these substructures are generally synthesized from azomethines *via* nucleophilic addition reactions for instance the Grignard-Barbier allylations³²⁻³⁵ and Strecker-type reactions.³⁶⁻⁴¹ The experimental process of the Strecker reaction is tedious and therefore, several modified procedures have been developed using different cyanide reagents (diethylaluminium cyanide, tri-*n*-butyltin cyanide, diethyl phosphorocyanidate, and trimethylsilyl cyanide⁴²) and catalysts such as lithium

Comentado [u1]: Which substructures? Also, allylation of imines affords allylic amines!

perchlorate,⁴³ vanadyl triflate,⁴⁴ zinc halides,⁴⁵ $H_{14}[NaP_5W_{30}O_{110}]$,⁴⁶ Montmorillonite KSF,³⁷ and indium trichloride.⁴⁷

In continuation of our previous studies on the synthesis of novel ionic liquids (ILs), molten salts (MSs), and phthalocyanine based catalysts and their application in multi component reactions (MCRs),⁴⁸ herein we introduce nano tetra-2,3-pyridiniumporphyrinato-oxo-vanadium tricyanomethanide $\{[VO(TPPA)][C(CN)_3]_4\}$ as a vanadium surface free phthalocyanine based molten salt catalyst for the Strecker synthesis of α -aminonitrile derivatives by a one-pot three-component reaction of aromatic aldehydes, trimethylsilyl cyanide (TMSCN), and aniline derivatives under neat conditions at 50 °C (Scheme 1).



Scheme 1. Synthesis of nano tetra-2,3-pyridiniumporphyrinato-oxo-vanadium tricyanomethanide $\{[VO(TPPA)][C(CN)_3]_4\}$ as a vanadium surface free phthalocyanine based molten salt catalyst and its application to the Strecker synthesis of α -aminonitriles.

2. Results and discussion

2.1. Characterization of nano tetra-2,3-pyridiniumporphyrinato-oxo-vanadium tricyanomethanide $\{[VO(TPPA)][C(CN)_3]_4\}$ as a phthalocyanine based molten salt catalyst.

Catalyst $\{[VO(TPPA)][C(CN)_3]_4\}$ was synthesized *via* the method described by Yokote et al. using urea, tetrahydrated ammonium molybdate $[(NH_4)_6Mo_7O_{24}.4H_2O]$, 2,3-pyridine-dicarboxylic acid, and vanadium (V) oxide.^{25a} The structure of tetra-2,3-pyridiniumporphyrinato-oxo-vanadium tricyanomethanide $\{[VO(TPPA)][C(CN)_3]_4\}$ was investigated and fully characterized *via* FT-IR, UV-Vis, XRD, XPS, SEM, HRTEM, EDX, ICP-MS, and TGA.

In the FT-IR spectrum of $\{[VO(TPPA)][C(CN)_3]_4\}$, the absorption bands at 991 and 622 cm^{-1} are related to the stretching vibrational modes of V=O. Additionally, the absorption bands at 1611 cm^{-1} (linked to C=N stretching) and at 1458 cm^{-1} (related to C=C stretching) were also observed in the IR spectrum of the catalyst. The known peaks at 2242, 2182, and 2082 cm^{-1} are linked to C≡N stretching group on tricyanomethanide counter ion. Also, the identified peaks at 3446, 3356, and 3204 cm^{-1} are connected to the N-H stretching absorptions of the pyridinium ring. A comparison of the FT-IR spectra of the catalyst with $\{[VO(TPPA)][C(CN)_3]_4\}$ catalyst in comparison with other substrates and $[VO(TPPA)]$ presented synthesis of catalyst (Fig. 1).

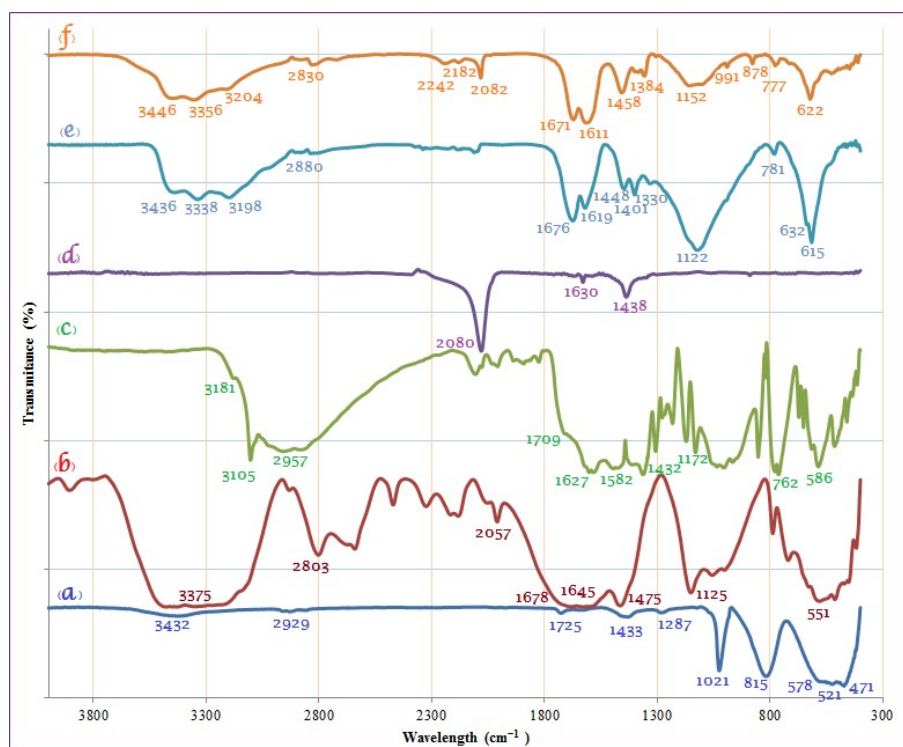


Fig. 1. FT-IR spectrum of (a) V₂O₅; (b) urea; (c) 2,3-pyridinedicarboxylic acid; (d) tricyanomethane; (e) [VO(TPPA)]; (f) {[VO(TPPA)][C(CN)₃]₄}.

The structure of {[VO(TPPA)][C(CN)₃]₄} was also studied and compared with [VO(TPPA)] by UV-visible spectroscopy. Thus, aqueous ethanol solutions (EtOH/H₂O: 10/1), of {[VO(TPPA)][C(CN)₃]₄} and [VO(TPPA)] were prepared and analyzed. As depicted in Figure 2, these compounds, showed strong absorption bands at 821 and 767 nm (visible region), respectively. Furthermore, the optical band-gap energies ($E_{bg} = 1240/\lambda_{max}$) for {[VO(TPPA)][C(CN)₃]₄} and [VO(TPPA)] were calculated, resulting 1.510 and 1.616 eV, respectively. It is important to underline, that while synthesizing {[VO(TPPA)][C(CN)₃]₄}, the

color of the aqueous reaction solution changed from green to pale green while adding tricyanomethanide counter ion (see experimental section). This acid-base behavior mechanism was found to be similar in UV-vis. spectrum as previously described [where? Reference?](#). Thus, the red shift differences in the absorption maximum between the catalyst and [VO(TPPA)] can be considered as proof of the formation of the catalyst.

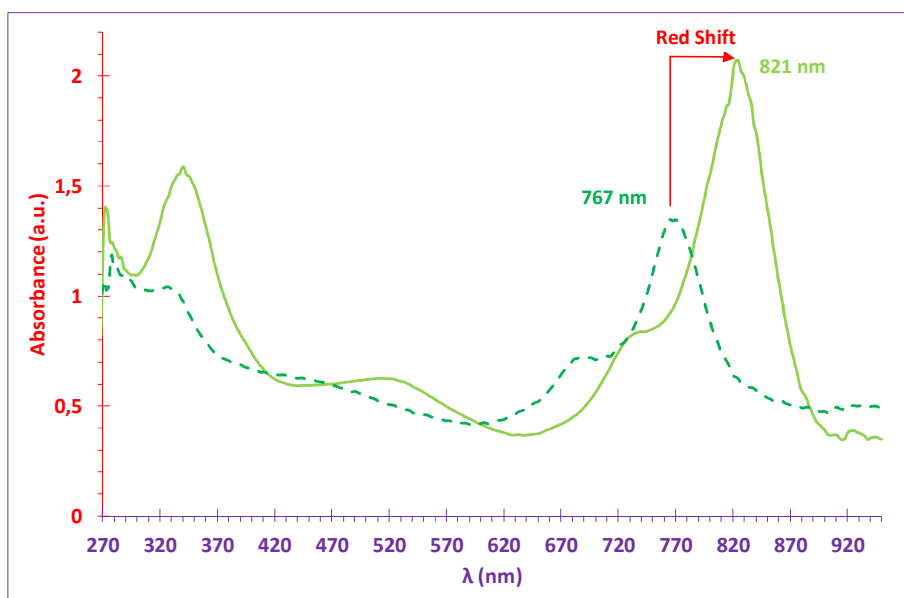


Fig. 2. UV-Vis. spectrum of {[VO(TPPA)][C(CN)₃]₄} pale green line (a) and [VO(TPPA)] green line dash (b).

The Metallic composition of {[VO(TPPA)][C(CN)₃]₄} and [VO(TPPA)] were determined by EDX, inductive coupling plasma mass spectrometry (ICP-MS) and thermogravimetric analysis (TGA).

The Energy-dispersive X-ray spectroscopy (EDX) data obtained from {[VO(TPPA)][C(CN)₃]₄} confirmed the presence of the anticipated elements in the structure of the catalyst: carbon (C), nitrogen (N), oxygen (O), and vanadium (V) (Fig. 3). No extra peaks

connected with any impurity were detected in the SEM coupled EDX, confirming the catalyst composition: C (22.84%), N (21.50%), O (34.07%), and V (0.27%). Moreover, a 0.08112% w/w catalyst vanadium content was determined by inductive coupling plasma mass spectrometry (ICP-MS). In addition, the vanadium content of the [VO(TPPA)] was also measured *via* ICP-MS, which displayed a value of 0.1659% w/w.

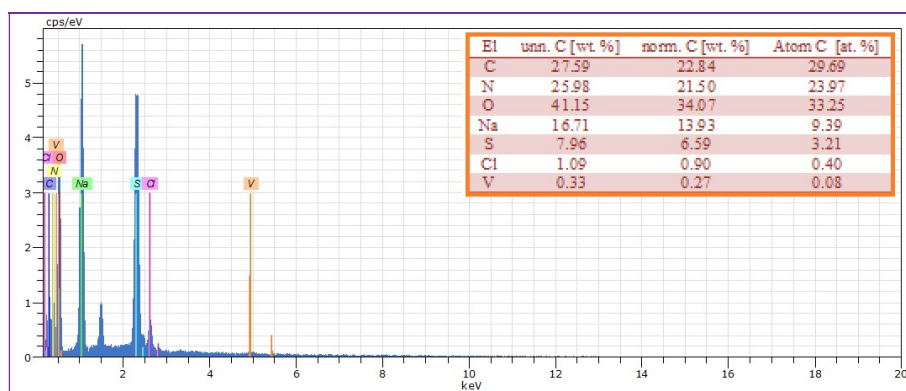
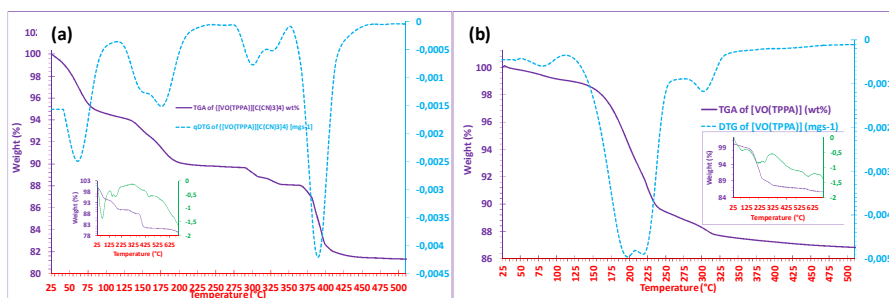


Fig. 3. The EDX spectroscopy of {[VO(TPPA)][C(CN)₃]₄} as a catalyst.

Figure 4 shows the thermal behavior of {[VO(TPPA)][C(CN)₃]₄} and [VO(TPPA)] under nitrogen atmosphere. The thermal gravimetric analysis (TGA), derivatives thermal gravimetric analysis (DTG), and the differential thermal analysis (DTA) of the catalyst was generally investigated.

The DTA analysis diagram shows a general negative downward slope between 25 °C to 700 °C in which, decomposition of catalyst and its precursor in nitrogen atmosphere were **exothermic**. Moreover, the TGA, DTG, and DTA thermal decomposition processes, as shown in figures 4a-c, included the following three steps. The first one, related to the removal of surface-adsorbed water and organic solvents, took place between 25 and 110 °C and involved a weight loss of 0.9 and 5.6% for [VO(TPPA)] and {[VO(TPPA)][C(CN)₃]₄}, respectively. The higher

percentage of absorbed water for catalyst when compared with its precursor could be reasoned for the ionic molten salt nature of $\{[\text{VO}(\text{TPPA})][\text{C}(\text{CN})_3]_4\}$. The second weight loss region shown between 110 to 405 °C was attributed to the continuing decomposition of the phthalocyanine ring. A weight loss of 10.2 and 4.7 wt% were observed for $[\text{VO}(\text{TPPA})]$ for $\{[\text{VO}(\text{TPPA})][\text{C}(\text{CN})_3]_4\}$, respectively. Finally, the third weight loss region for $\{[\text{VO}(\text{TPPA})][\text{C}(\text{CN})_3]_4\}$ (between 405 to 510 °C) could be ascribed to the continuing decomposition of the ionic (pyridinium/tricyanomethanide) moieties of the catalyst. On the contrary, no distinct weight loss was detected in this temperature range for $[\text{VO}(\text{TPPA})]$, suggesting a non-ionic composition of this material. The weight loss for this third step was calculated to be lower than 0.1% for $[\text{VO}(\text{TPPA})]$ and 8.5% for $\{[\text{VO}(\text{TPPA})][\text{C}(\text{CN})_3]_4\}$. In addition, above 700 °C, it was not observed any significant weight loss. As it is clearly indicated in Figure 4c for the results of the DTG analysis, the thermal stability of the catalyst was improved from 110-405 °C to 405-510 °C when compared with its precursor, which could be attributed to the ionic character of the pyridinium functional groups.



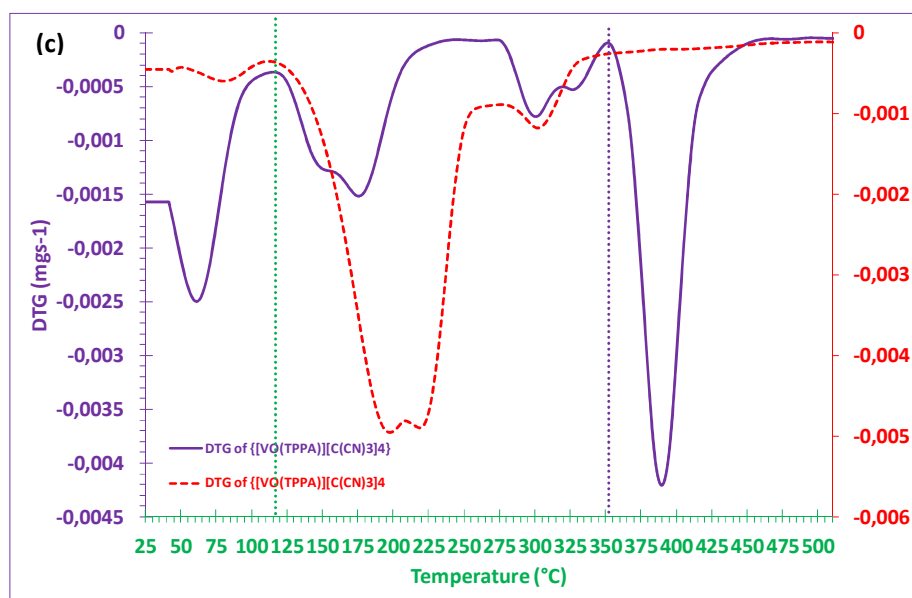


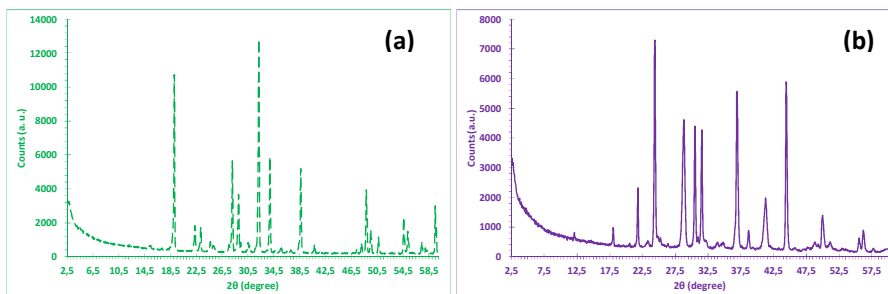
Fig. 4. Thermal gravimetric analysis (TGA/DTG) and inlet (TGA/DTA) of $\{[VO(TPPA)][C(CN)_3]_4\}$ (a); thermal gravimetric analysis (TGA/DTG) and inlet (TGA/DTA) of $[VO(TPPA)]$ (b); comparing superimposed derivative thermal gravimetric (DTG) of both $\{[VO(TPPA)][C(CN)_3]_4\}$ and $[VO(TPPA)]$ (c)

The particle size and shape as well as the morphology of $\{[VO(TPPA)][C(CN)_3]_4\}$ and $[VO(TPPA)]$ were studied by XRD, SEM, and HRTEM (Figures 5-7). Characterization by X-ray diffraction (XRD) was performed to investigate the crystalline structure of $\{[VO(TPPA)][C(CN)_3]_4\}$ and $[VO(TPPA)]$ in a range of $2\theta = 2.5-60^\circ$ (Fig. 5). The XRD analysis revealed thirteen characteristic peaks for the catalyst between 18.05° and 56.20° . The peak width (FWHM), size, and inter planar distance from the XRD pattern of the catalyst were studied and the achieved results are summarized in Table 1. A similar analysis for $[VO(TPPA)]$ is summarized in Table 2. These characteristic peaks indicate crystallographic planes of catalyst. The broad peak ($2\theta = 24.40^\circ$) displays the nanometer-sized crystallines. In addition the average

crystalline size D [nm] of catalyst can be estimated according to the Scherrer equation [$D = K\lambda/(\beta\cos\theta)$] where λ is the wavelength of Cu k_{α} (1.5405 Å) as the X-ray source, K is a shape factor with the value of 0.9, θ is the Bragg diffraction angle and β is the full width at half maximum (FWHM) of the peak in radians. The calculated average particle size for $\{[\text{VO}(\text{TPPA})][\text{C}(\text{CN})_3]_4\}$ and $[\text{VO}(\text{TPPA})]$ is summarized in Tables 1 and 2, respectively. On the other hand, the averaged inter-planar distance [nm] of $\{[\text{VO}(\text{TPPA})][\text{C}(\text{CN})_3]_4\}$ and $[\text{VO}(\text{TPPA})]$ were calculated according to the Bragg equation: $d_{hkl} = \lambda/(2\sin\theta)$, where K is a shape factor with the value of 0.9, θ is the Bragg diffraction angle, λ is the wavelength of Cu k_{α} (1.5405 Å) as the X-ray source. **Discuss the results of the Table??**

Comentado [u2]: Too long sentence. We do not understand the meaning. Please rewrite it.

Moreover, The crystalline diffraction lines of $\{[\text{VO}(\text{TPPA})][\text{C}(\text{CN})_3]_4\}$, showed different angle to those of $[\text{VO}(\text{TPPA})]$, as depicted in Figure 5c where the superimposed XRD spectra of both materials is shown.



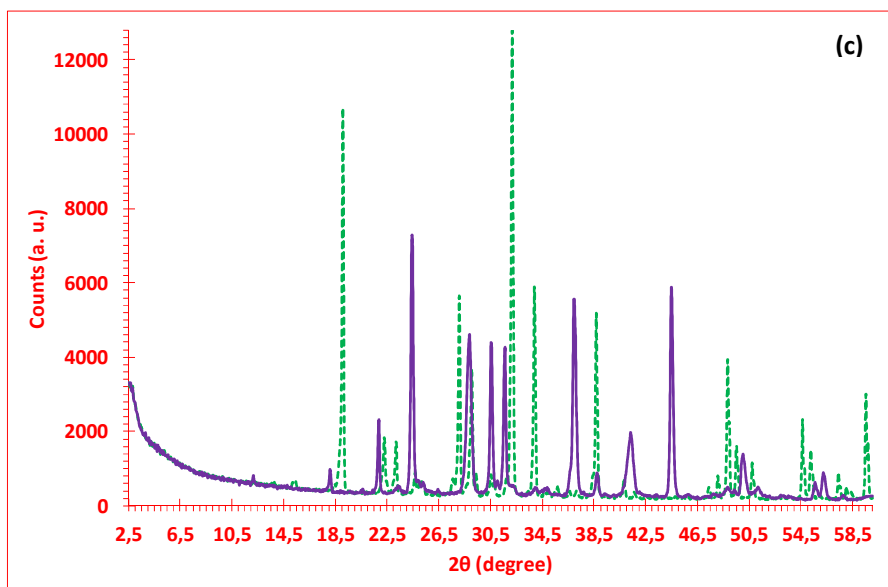


Fig. 5. X-ray diffraction (XRD) pattern of [VO(TPPA)] (a); {[VO(TPPA)][C(CN)₃]₄} (b) mixture of [VO(TPPA)] (green with dash line) and {[VO(TPPA)][C(CN)₃]₄} (violet line) (c).

Table 1. X-ray diffraction (XRD) data for {[VO(TPPA)][C(CN)₃]₄}.

Entry	2θ	Peak width [FWHM] (degree)	Size [nm]	Inter planer distance [nm]
1	18.05	0.34	23.66	0.490868
2	21.85	0.25	32.37	0.406172
3	24.40	0.27	30.11	0.364368
4	28.85	0.45	18.23	0.309098
5	30.50	0.22	37.43	0.292741
6	31.60	0.20	41.28	0.282797
7	36.90	0.27	31.02	0.243304
8	38.70	0.36	23.39	0.232391
9	41.30	0.59	14.39	0.218342

10	44.45	0.26	33.01	0.203572
11	49.90	0.44	19.91	0.182539
12	55.55	0.41	21.90	0.165236
13	56.20	0.39	23.10	0.163478

Table 2. X-ray diffraction (XRD) data for [VO(TPPA)].

Entry	2 θ	Peak width [FWHM] (degree)	Size [nm]	Inter planer distance [nm]
1	19.05	0.15	53.70	0.465319
2	22.25	0.23	35.21	0.399067
3	23.15	0.23	35.26	0.383753
4	28.05	0.17	48.25	0.317729
5	29.00	0.20	41.03	0.307533
6	32.15	0.10	82.81	0.278084
7	33.90	0.21	39.56	0.264117
8	38.65	0.18	46.78	0.232680
9	48.80	0.24	36.35	0.186394
10	49.45	0.24	36.44	0.184095
11	50.80	0.25	35.17	0.179845
12	54.60	0.14	63.87	0.167884
13	55.20	0.29	30.91	0.166200
14	59.50	0.14	65.37	0.155174
15	59.55	0.31	29.53	0.155056

The surface texture and morphological properties of the catalyst were also studied using scanning electron microscopy (SEM, Figure 6) and high-resolution transmission electron microscopy (TEM, Figure 7). As depicted, both analyses showed that it's with near fine fibrillar morphology were prepared with suitable monodispersity. The catalyst synthesis employed in this

Comentado [u3]: Please rewrite. We do not catch the meaning.

investigation produced a uniformly dispersion of small particles with 14.39-41.28 nm average size, which was in accordance with the results obtained by XRD studies. Moreover, in combination with SEM, wavelength-dispersive X-ray spectroscopy (WDX) provided qualitative information about the distribution of different chemical elements in the catalyst matrix. Fig. 6 collects representative SEM and elemental maps (WDX) images for the produced catalyst. It can be seen that vanadium metal particles are finely dispersed in the material. The chosen-area elemental analysis figure exposes the presence of C, N, O and V by the sample in a homogeneous procedure, which approves the regular uniformity of the synthesized catalyst. Moreover, The XRD pattern changes of {[VO(TPPA)][C(CN)₃]₄} catalyst in comparison with [VO(TPPA)] presented production of catalyst (Fig. 5).

Comentado [u4]: Please put some order in the discussion. You talked about XRD and then SEM and then again XRD. Also, we do not understand the first sentence. Please rewrite it.

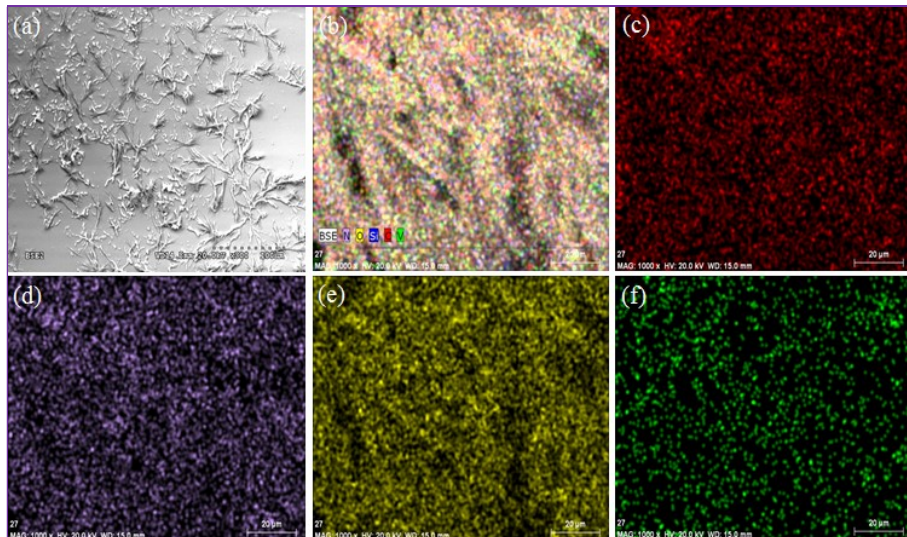


Fig. 6. Scanning electron microscopy (SEM) of $\{[\text{VO}(\text{TPPA})][\text{C}(\text{CN})_3]_4\}$ (a); elemental maps (WDX) of $\{[\text{VO}(\text{TPPA})][\text{C}(\text{CN})_3]_4\}$ (b) and displays of C (c), N (d), O (e), and V (f) atom in the catalyst.

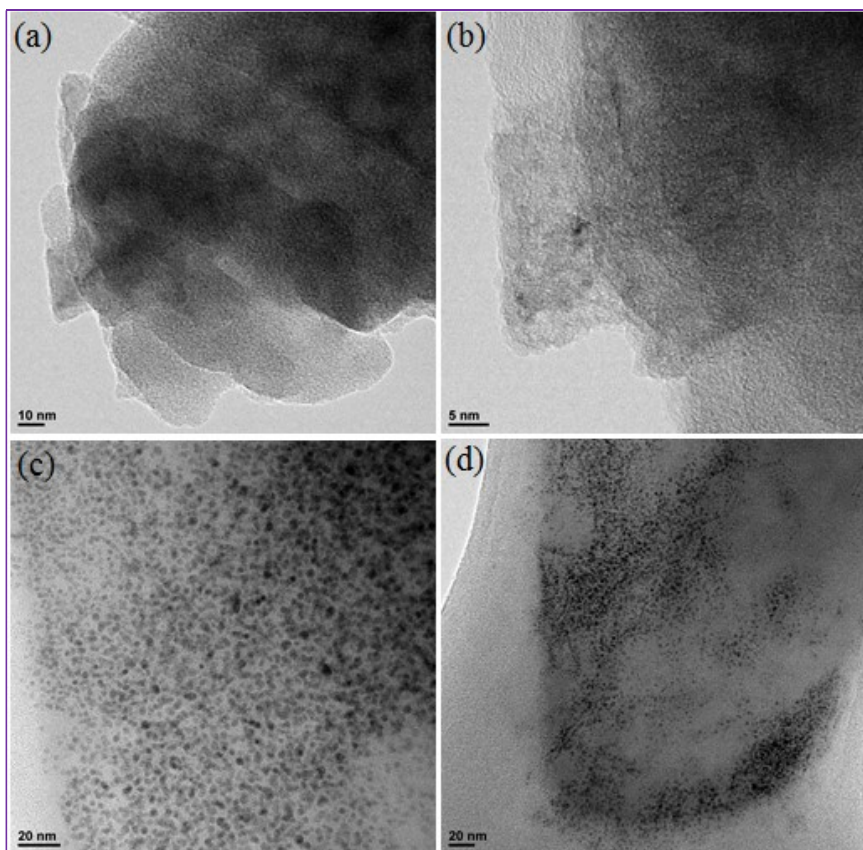


Fig. 7. High resolution transmission electron microscopy (HRTEM) of $[\text{VO}(\text{TPPA})]$ (a and b) and $\{[\text{VO}(\text{TPPA})][\text{C}(\text{CN})_3]_4\}$ (c and d).

X-ray photoelectron spectroscopy (XPS) studies were next performed over $\{[\text{VO}(\text{TPPA})][\text{C}(\text{CN})_3]_4\}$ and $[\text{VO}(\text{TPPA})]$ in order to get insight about the surface composition of these materials. As depicted in Figure 8a for $[\text{VO}(\text{TPPA})]$ (red and blue lines), the V2p peaks

could be fitted into the two different peaks located at 516.39 and 523.89 eV (in red) corresponding to $2p^{3/2}$ and $2p^{1/2}$ level with a relative area of 1 to 0.52, respectively. Moreover, blue residuals lines located at 523.48 eV. On the other hand $\{[VO(TPPA)][C(CN)_3]_4\}$ (Figure 8a, violet and orange lines), the violet peaks for vanadium $2p^{3/2}$ and $2p^{1/2}$ were not detected, plus a orange residuals lines located at 522.68 eV. Since the ICP-MS, EDX and elemental mapping analyses had previously approved the presence of vanadium in both $\{[VO(TPPA)][C(CN)_3]_4\}$ and $[VO(TPPA)]$, this result suggested the absence of vanadium oxide on the surface of the catalyst.⁵⁶ Moreover, the C1s XPS spectrum of $[VO(TPPA)]$ (Figure 8b, red lines) could be deconvoluted into three peaks at 286.64, 285.74, and 288.54 eV, revealing the existence of C=C, C=N, and N-C=N moieties, respectively (ratio: 1/0.55/0.63). However, compared with $[VO(TPPA)]$, the binding energy of C=N and N-C=N of $\{[VO(TPPA)][C(CN)_3]_4\}$ shifted to 285.84 and 288.71 eV. This positive shift of the binding energy suggested the presence of pyridinium NH^+ moieties. In addition, Figures 5a,b also showed the reduction of the C=N (0.55 to 0.23) and N-C=N (0.63 to 0.30) functional groups in the catalyst when compared with the precursor.

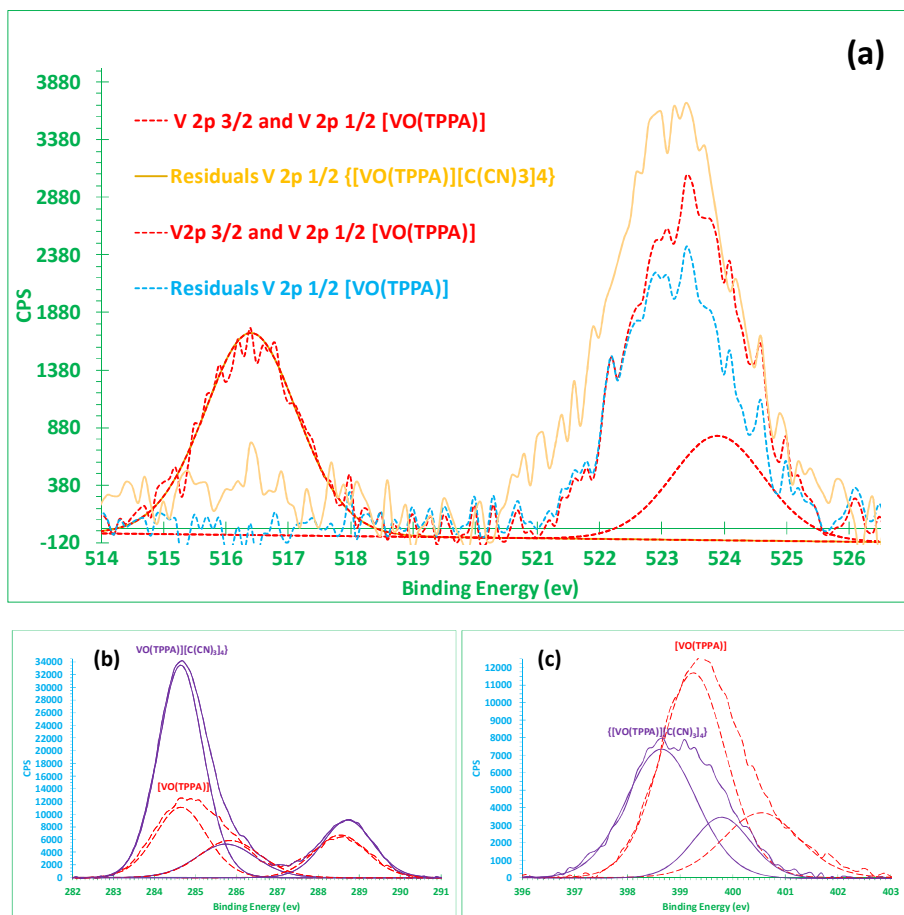


Fig. 8. High-resolution XPS spectra of V2p (a) in [VO(TPPA)] (red lines with blue residuals lines) and in {[VO(TPPA)][C(CN)₃]₄} (orange residuals lines); XPS spectra of C1s (b) in [VO(TPPA)] (red dash lines) and in {[VO(TPPA)][C(CN)₃]₄} (violet lines); and XPS spectra of N1s (c) in [VO(TPPA)] (red dash lines) and in {[VO(TPPA)][C(CN)₃]₄} (violet lines).

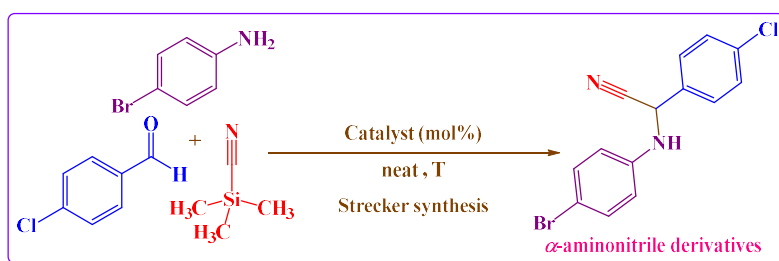
2.2. Application of nano tetra-2,3-pyridiniumporphyrinato-oxo-vanadium tricyanomethanide $\{[VO(TPPA)][C(CN)_3]_4\}$ as a phthalocyanine based molten salt catalyst for the Strecker synthesis of α -aminonitriles.

In continuation of our studies⁴⁸ related with the applications of $\{[VO(TPPA)][C(CN)_3]_4\}$ in organic synthesis, we next studied the use of this catalyst in the Strecker synthesis of α -aminonitriles (Scheme 1). To find simple and appropriate conditions for the Strecker synthesis of α -aminonitriles, we performed the corresponding optimization on a model reaction between 4-chlorobenzaldehyde (1 eq.) and 4-bromoaniline (1 eq.) in the presence of TMSCN (1.5 eq.).

Please discuss the Table in order! From entry 1 to entry 20. In order to the optimizing of reaction conditions, the reaction was studied using linked different catalyst under neat conditions. The use of 50 mg of $\{[VO(TPPA)][C(CN)_3]_4\}$ under these conditions provided a 88% yield (Table 3, entry 13) of the desired product. Optimization of the reaction conditions was undertaken to increase the yield employing various amounts of catalyst. The yield was increased to 91% using 10 mg or 20 mg of catalyst (Table 3, entries 1 and 12). However, the addition of 100 mg of the catalyst was found to have an inhibitory effect on the production of the α -aminonitriles (Table 3, entry 14), while a reduction in yield was detected by decreasing the catalyst loading to 5 mg (Table 3, entry 11). The influence of other catalysts was also examined. With NH_2SO_3H , $Ce(HSO_4)_3 \cdot 7H_2O$ and $NaCl$ the reaction did not proceed (Table 3, entries 3, 8 and 20) and whereas with other catalysts the isolated yield of desired product was appropriate attained. The results achieved with other catalysts are summarized in Table 3. Also, and in absence of catalyst for a model reaction the desired product was not prepared (Table 3, entry 15). Other catalysts were not efficient under the similar condition, therefore $\{[VO(TPPA)][C(CN)_3]_4\}$ was chosen as the best catalyst among all. Next, the effect of temperature on rate of reaction was

investigated at different temperatures. When the reaction was performed at 50 °C, the maximum yield was obtained in a short reaction time (Table 3, entry 1). Furthermore, increasing the temperature more than 50 °C has no change on the yield or reaction time (Table 3, entries 17 and 18). Also, it was found that at room temperature, the reaction was very slow and did not progress to completion (Table 3, entry 16).

Table 3. Reaction conditions optimization of the Strecker synthesis under neat conditions.^a



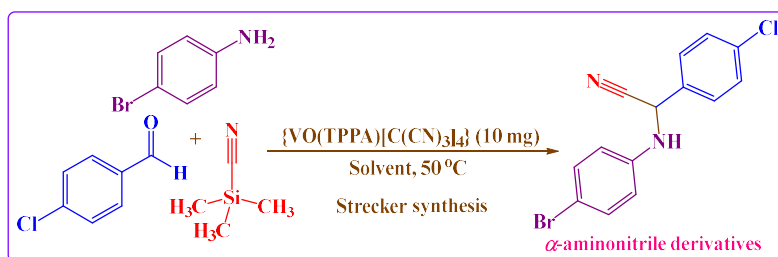
Entry	Catalyst	Catalyst loading (mol%)	Reaction temperature (°C)	Time (min)	Yield ^b (%)
1	{[VO(TPPA)][C(CN) ₃] ₄ }	0.016	50	20	91
2	[Msim]Cl	2	50	30	85
3	NH ₂ SO ₃ H	10	50	45	–
4	[MIMPS] ₃ PW ₁₂ O ₄₀	2	50	30	87
5	H ₃ PW ₁₂ O ₄₀	5	50	30	78
6	Acetic acid	20	50	45	53
7	[Dsim]Cl	2	50	30	85
8	Ce(HSO ₄) ₃ ·7H ₂ O	20	50	45	–
9	[TEAPS] ₃ PW ₁₂ O ₄₀	2	50	30	85
10	HBF ₄	10	50	30	61
11	{[VO(TPPA)][C(CN) ₃] ₄ }	0.008	50	30	75
12	{[VO(TPPA)][C(CN) ₃] ₄ }	0.032	50	20	91

13	$\{[\text{VO}(\text{TPPA})][\text{C}(\text{CN})_3]_4\}$	0.08	50	20	88
14	$\{[\text{VO}(\text{TPPA})][\text{C}(\text{CN})_3]_4\}$	0.16	50	20	85
15	Catalyst-free	–	50	60	–
16	$\{[\text{VO}(\text{TPPA})][\text{C}(\text{CN})_3]_4\}$	0.016	r.t.	30	57
17	$\{[\text{VO}(\text{TPPA})][\text{C}(\text{CN})_3]_4\}$	0.016	75	20	91
18	$\{[\text{VO}(\text{TPPA})][\text{C}(\text{CN})_3]_4\}$	0.016	100	20	91
19	$[\text{VO}(\text{TPPA})]$	0.032	50	30	88
20	NaCl	0.5	50	60	–

^aReaction conditions: 4-chlorobenzaldehyde (1 mmol; 140 mg), TMSCN (1.5 mmol; 149 mg; 188 μL), 4-bromoaniline (1 mmol; 172 mg); ^bIsolated yield.

Next, we carried out an optimization of the reaction media (Table 4). Generally, polar solvents led to higher yields than non-polar ones. However, as depicted in entries 1-7, the use of solvent is detrimental for the reaction yield. Finally, it was detected that neat conditions afforded the best result in terms of reaction time and yield (Table 4, entry 8) probably due to a more intimate contact between the reactants and the catalyst surface under these conditions.

Table 4. $\{[\text{VO}(\text{TPPA})][\text{C}(\text{CN})_3]_4\}$ -catalyzed Strecker reaction. Solvent optimization.^a



Entry	Solvent	Time (min)	Yield ^b (%)
1	H ₂ O	30	84

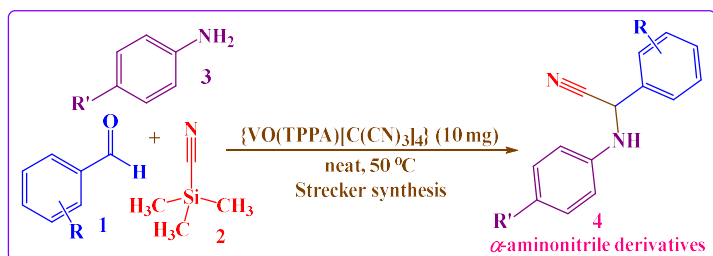
2	C ₂ H ₅ OH	30	87
3	CH ₃ CN	30	81
4	CH ₃ CO ₂ Et	45	75
5	CH ₂ Cl ₂	45	68
6	Toluene	60	51
7	<i>n</i> -Hexane	60	45
8	neat	20	91

^aReaction conditions: 4-chlorobenzaldehyde (1 mmol; 140 mg), TMSCN (1.5 mmol; 149 mg; 188 μ L), 4-bromoaniline (1 mmol; 172 mg); ^bIsolated yield.

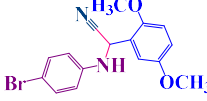
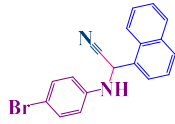
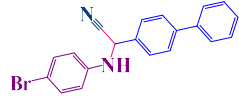
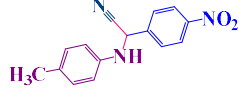
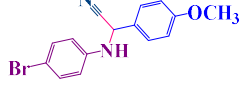

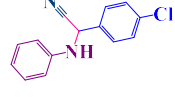
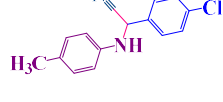
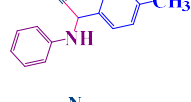
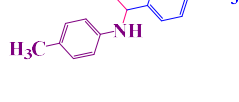
To study the versatility and generality of the optimized process, the reaction was extended to different aromatic aldehydes. The results are summarized in Table 5. It was obvious that the product yield was influenced by both electronic and steric effects of the substituted groups. Aromatic aldehydes with electron-donating groups gave lower yields than those bearing electron-withdrawing substituents. Additionally, the effect of steric hindrance on the aromatic aldehydes was important. In general, *ortho*-substituted aromatic aldehydes provided lower yields. On the other hand, hetero-aromatic aldehydes required longer reaction times than aromatic aldehydes affording lower yields as well.. The structures of α -aminonitriles were approved from ¹H NMR, ¹³C NMR, GC-MS, and FT-IR spectral data. In order to evaluate the efficacy of {[VO(TPPA)][C(CN)₃]₄} as a catalyst on the Strecker synthesis of α -aminonitrile derivatives, TOF values were also calculated (according to the ICP-MS results, 10 mg of catalyst are equivalent to 0.016 mol% of catalyst). Furthermore, in this reaction condition 4-bromoaniline reacted faster than 4-methylaniline and aniline. Moreover, In the presence of terephthalaldehyde as an aldehyde derivative, α -bisaminonitrile products were produced (Table 5, entry 15 and 17). No by-products from the cyanide addition to the aldehydes were detected in the crude reaction mixtures due to the rapid activation of the in situ produced imine by the catalyst.⁴⁹⁻⁵¹

Please discuss longer the results and in order of appearance! Also, there is no sense to say that the TOF was determined and no comments are included, for instance compare the TOF number of this catalyst with those reported for other catalysts.

Table 5. {[VO(TPPA)]C(CN)₃]₄}-catalyzed Strecker synthesis of α -aminonitrile derivatives under neat conditions at 50 °C.^a



Entry	Product	M.p (°C) (color) ^{Ref.}	Time (min)	Yield ^b (%)	TOF
1		337-339 (Yellow solid) ⁵⁵	20	91	284.4
2		33-35 (Red solid) ⁴⁹	25	90	225.0
3		178-180 (Yellow solid)	30	88	183.3
4		303-305 (Orange solid) ⁵⁵	15	93	387.5

5		4e	253-255 (Yellow solid)	30	86	179.2
6		4f	156-158 (Yellow solid)	25	90	225.0
7		4g	151-153 (Yellow solid)	25	91	227.5
8		4h	87-89 (Red solid) ⁴⁹	20	91	284.4
9		4i	146-148 (Yellow solid)	30	89	185.4
10		4j	263-265 (Yellow solid)	25	90	225.0
11		4k	110-112 (Brown solid) ⁴⁹	30	87	181.3
12		4l	87-89 (Brown solid) ⁵²	25	89	222.5
13		4m	73-75 (Green solid) ⁴⁹	40	85	132.8
14		4n	105-107 (Green solid) ⁴⁹	35	87	155.4

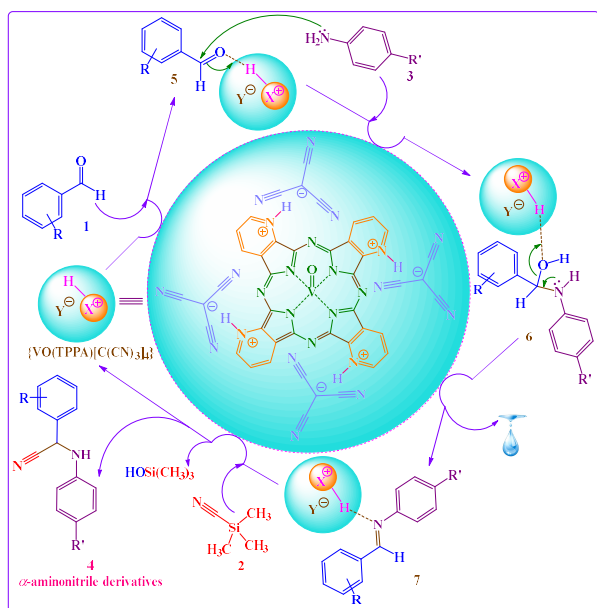
15		4o	161-163 (Yellow solid) ⁵³	30	88	183.3
16		4p	105-107 (Red solid) ⁵⁴	35	86	153.6
17		4q	194-196 (Yellow solid)	25	90	225.0
18		4r	238-240 (Yellow solid)	30	89	185.4
19		4s	218-220 (Yellow solid) ⁵⁵	30	89	185.4
20		4t	253-255 (Yellow solid)	30	85	177.1
21		4u	83-85 (Green solid) ⁴⁹	45	85	118.1
22		4v	106-108 (Green solid) ⁴⁹	40	87	135.9

Reaction conditions: ^aAldehyde (1 mmol), TMSCN (1.5 mmol; 149 mg; 188 μ L), aniline derivatives (1 mmol);

^bIsolated yield.

According to our studies on the catalyst and previous studies (which ones?, reference?), we present a plausible pathway for the Strecker synthesis of α -aminonitriles in the presence of

$\{[\text{VO}(\text{TPPA})][\text{C}(\text{CN})_3]_4\}$ as a vanadium surface free phthalocyanine based molten salt catalyst in Scheme 2. Thus, in the absence of vanadium oxide in the surface of the catalyst, the pyridinium NH^+ moieties of $\{[\text{VO}(\text{TPPA})][\text{C}(\text{CN})_3]_4\}$ activate the carbonyl group of the aromatic aldehydes **1** via hydrogen bonding towards nucleophilic attack of the aniline derivatives **3**. This reaction would produce the corresponding imines **7**, process promoted by the water physically and/or chemically adsorbed on the catalyst surface. In the next step, a similar catalyst hydrogen-bonding activation on both the generated imine **7** and TMSCN (by generation of pentacoordinated Si) takes place affording the corresponding α -aminonitriles **4** and trimethylsilanol (Scheme 2).



Scheme 2. Plausible mechanism for the Strecker synthesis of α -aminonitriles using $\{[\text{VO}(\text{TPPA})][\text{C}(\text{CN})_3]_4\}$ as a phthalocyanine based molten salt catalyst.

The recyclability of the catalyst was also investigated by running seven consecutive cycles of the model synthesis of **4a**. It is important to underline, that the reaction product can be simply separated from the catalyst based on solubility issues (see experimental section). Then, after each run, the catalyst was filtered, exhaustively washed with ethanol (where the products are soluble but not the catalyst) and finally dried. As seen in Fig. 9, the $\{[\text{VO}(\text{TPPA})][\text{C}(\text{CN})_3]_4\}$ catalyst promoted the reactions without significant loss of catalytic activity. FT-IR analysis of $\{[\text{VO}(\text{TPPA})][\text{C}(\text{CN})_3]_4\}$ after the **xx** run, confirmed the stability of the nano catalyst during the recycling procedure.

Comentado [u5]: Which cycle?

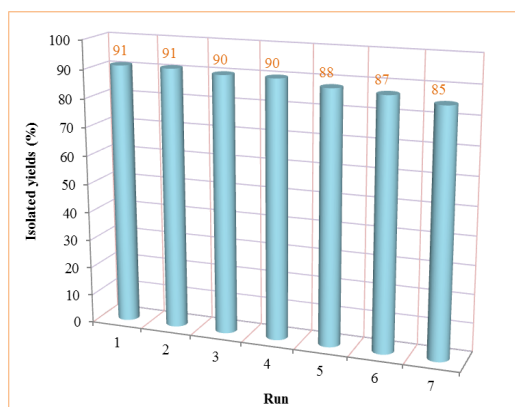


Fig. 9. Reusability studies of the $\{[\text{VO}(\text{TPPA})][\text{C}(\text{CN})_3]_4\}$ as a phthalocyanine based molten salt catalyst for the Strecker synthesis of α -aminonitrile **4a**.

3. Conclusion

We have synthesized and fully characterized (FT-IR, UV-Vis, XRD, XPS, SEM, HRTEM, EDX, ICP-MS, and TG analyses) a nano tetra-2,3-pyridiniumporphyrinato-oxovanadium tricyanomethanide $\{[\text{VO}(\text{TPPA})][\text{C}(\text{CN})_3]_4\}$ as a vanadium surface free

phthalocyanine based molten salt which is an efficient and recyclable catalyst for the Strecker synthesis of α -aminonitriles. The reported one-pot synthesis of α -aminonitriles is a suitable alternative to multi-step methodologies and offers different advantages such as, wide functional group tolerance, high reaction rates and yields, neat conditions, and use of a stable and recyclable catalyst.

Experimental

3.1. General information.

All used chemicals and solvents were of reagent grade and purchased from Sigma-Aldrich, Fluka, Merck, and Across Organic Chemical Companies. All reagents were used without any further purification. TLC analysis was performed on a UV-active aluminium-backed F254 silica gel plates. Melting points were measured with a Thermo Scientific apparatus and they were not corrected. Centrifugation procedures were performed in a Hettich-Universal centrifuge. Fourier transform-infrared spectra (FT-IR) were recorded on a Perkin-Elmer FT-IR spectrometer 17259 using KBr disks. Ultraviolet-visible spectra were recorded on a Perkin-Elmer UV-Vis Spectrophotometer 35. The samples (10 mg) for UV/Vis study were prepared in ethanol (xx mL) by dispersing procedure. ^1H NMR (400 MHz or 300 MHz) spectra were obtained on a Bruker Avance 400 or 300 NMR spectrometers, respectively, in proton coupled mode using deuterated DMSO as a solvent, unless otherwise stated. ^{13}C NMR (101 MHz) spectra were acquired on a Bruker Avance 400 NMR spectrometer in proton decoupled mode at 20 °C in deuterated DMSO as solvent, unless otherwise stated. Chemical shifts are given in δ (parts per million) and the coupling constants (J) in hertz. Data for ^1H NMR are reported as follows: chemical shift (ppm), multiplicity (s, singlet; d, doublet; t, triplet; q, quartet; m, multiplet; and br, broad), coupling constant (Hz), and integration. Melting points were recorded on Buchi B-545 apparatus in open

Comentado [u6]: Which apparatus was used for the mp determination?

Comentado [u7]: Which apparatus was used for the mp determination?

capillary tubes. Thermogravimetric analyses (TGA) were carried out on a METTLER TOLEDO apparatus (models TGA/SDTA851 and /SF/1100 TG/DTA). Thermogravimetric analysis (TGA) was performed under a nitrogen atmosphere at 25°C and using heating rate of 20 °C min⁻¹ up to 700 °C. High resolution transmission electron microscopy (HRTEM) images were performed using a JEOLJEM-2010 microscope operating at an accelerating voltage of 200 kv. Samples were prepared by drop casting the dispersed particles onto a 200-mesh copper grid coated with a holey carbon film. Scanning electron microscopy (SEM) studies were performed using a Hitachi S3000N, equipped with an X-ray detector Bruker XFlash 3001 for microanalysis (EDX) and mapping (WDX). X-ray diffraction (XRD) analyses were performed using a Bruker D8-Advance apparatus using a monochromatized Cu K α (λ = 0.154nm) X-ray source in the range 5° < 2 θ < 60°. Low resolution mass spectra (EI) were obtained at 70 eV using an Agilent 5973 Network spectrometer, with fragment ions m/z reported with relative intensities (%) in parentheses. Inductive coupling plasma mass spectrometer (ICP-MS) was performed on an Agilent 7700x apparatus equipped with HMI (high matrix introduction) and He mode ORS as standard. Vanadium contents of {[VO(TPPA)][C(CN)₃]₄} and [VO(TPPA)] were determined using 2ml HNO₃ for 24h with constant stirring, filtration and diluted to 5ml with dionized water. X-ray photoelectron spectroscopy (XPS, K-ALPHA, Thermo Scientific) was used to analyze the samples surface. All spectra were collected using Al-K radiation (1486.6 eV), monochromatized by a twin crystal monochromator, yielding a focused X-ray spot (elliptical in shape with a major axis length of 400 μ m) at 3 mA \times 12 kV. The alpha hemispherical analyzer operated in the constant energy mode with survey scan pass energies of 200 eV to measure the whole energy band and 50 eV in a narrow scan to selectively measure the particular elements. XPS data were analyzed using Thermo Scientific Avantage Software. A smart background function was used to

approximate the experimental backgrounds and surface elemental composition was calculated from background-subtracted peak areas. Charge compensation was achieved with the system flood gun that provides low energy electrons and low energy argon ions from a single source.

3.2. General procedure for the synthesis of nano tetra-2,3-pyridiniumporphyrinato-oxovanadium tricyanomethanide {[VO(TPPA)][C(CN)₃]₄}.

{[VO(TPPA)][C(CN)₃]₄} was synthesized *via* the method described by Yokote et al.^{25a} Urea (13 g), ammonium molybdate [(NH₄)₆Mo₇O₂₄·4H₂O] (92 mg), 2,3-pyridine-dicarboxylic acid (2 g), and vanadium (V) oxide [V₂O₅] (200 mg) were grounded under neat conditions until an homogeneous mixture was obtained. The mixture was placed in a heating mantle, sealed and heated at 200-210 °C for 5 h. Then, the mixture was allowed to cool to room temperature over a 5 h period. The crude green solid obtained product (10.25 g) was crushed and washed consecutively with warm water, a warm aqueous NaOH solution (5% w/v), warm water, a warm diluted aqueous hydrochloric acid (2.5% v/v), and finally with warm water. The obtained crude product was dried at 100 °C under vacuum and finally purified through dissolving in concentrated sulphuric acid and pouring the solution into ice-water. The precipitated product was collected *via* centrifugation (ca. 200 r.p.m./10 min) and transferred to a fine glass sinter funnel where the mass was carefully washed with hot water, a warm aqueous sodium carbonate solution and finally with warm water. [VO(TPPA)] was dried at 100 °C under vacuum (isolated yield 67%; M.p.: 278-280 °C) (Scheme 1). The vanadium content of the [VO(TPPA)] was measured *via* ICP-MS, which displayed value of about 0.1659% w/w.

In the next step, to a round-bottomed flask (50 mL) containing a tricyanomethane (4 mmol; 360 mg) aqueous solution (xx mL water), [VO(TPPA)] (1 mmol, 31 mg) was added and stirred over a period of 5 h under reflux conditions. The obtained pale green solid

{[VO(TPPA)][C(CN)₃]₄} product was washed three times with diethyl ether, and then dried under vacuum (isolated yield 91%) (Scheme 1). {[VO(TPPA)][C(CN)₃]₄} (melting point: 225-227 °C was fully characterized by FT-IR, UV-Vis, XRD, XPS, SEM, HRTEM, EDX, ICP-MS, and TG analysis. **Compounds x, xx, xxx are known and the**

3.3. General procedure for the Strecker synthesis of α -aminonitrile derivatives using {[VO(TPPA)][C(CN)₃]₄} as a phthalocyanine based molten salt catalyst.

{[VO(TPPA)][C(CN)₃]₄} (10 mg) was added to a mixture of the corresponding aldehyde (1 mmol), TMSCN (1.5 mmol; 149 mg; 188 μ L) and the corresponding aniline derivative (1 mmol). The resulting mixture was stirred at 50 °C under neat conditions and the progress of the reaction was studied by TLC (*n*-hexane/ethyl acetate: 5/2). Once the reaction was finished, the catalyst was filtered and carefully washed with ethanol and then dried under vacuum (the products are soluble in ethanol but the {[VO(TPPA)][C(CN)₃]₄} is insoluble). The recycled catalyst was tested in the next run for the model reaction. The organic solvent was evaporated and the crude product was purified by a short column of silica gel using (*n*-hexane/ethyl acetate: 20/1) to yield the corresponding pure products.

What about the rest of the products? Are they known? We should mention all known compounds with the corresponding references.

3.4. Selected spectral data analysis for compounds

2-((4-bromophenyl)amino)-2-(3,4-dimethoxyphenyl)acetonitrile (4c).

Isolated as yellow solid, (305 mg, 88%), Melting point: 178–180 °C; **IR (KBr): ν (cm⁻¹) =**
¹H NMR (300 MHz) δ 7.37 – 7.31 (m, 2H), 7.16 – 7.09 (m, 2H), 7.04 (d, *J* = 9.0, 1H), 6.84 – 6.76 (m, 3H), 5.87 (d, *J* = 9.2, 1H), 3.78 (2s, 6H); ¹³C NMR (101 MHz) δ 149.7, 149.4, 145.8, 132.0, 127.3, 120.1, 119.9, 116.3, 112.2, 111.3, 109.8, 56.0, 48.3; MS (EI) *m/z* (%): **348 (*M*⁺+2,**

100), 346 (M^+ , 100), 320 (21), 218 (24), 207 (14), 179 (12), 176 (54), 165 (17), 157 (10), 155 (10), 78 (22), 76 (10), 63 (26).

2-((4-bromophenyl)amino)-2-(2,5-dimethoxyphenyl)acetonitrile (4e).

Isolated as yellow solid, (298 mg, 86%), Melting point: 253–255 °C; IR (KBr): ν (cm^{-1}) =

^1H NMR (400 MHz) δ 7.34 – 7.28 (m, 2H), 7.11 (d, J = 3.0, 1H), 7.05 (d, J = 9.0, 1H), 6.97 (dd, J = 9.0, 3.0, 1H), 6.80 – 6.75 (m, 2H), 6.72 (d, J = 9.2, 1H), 5.83 (d, J = 9.2, 1H), 3.79 (s, 3H), 3.71 (s, 3H); ^{13}C NMR (75 MHz) δ 153.6, 150.9, 145.5, 132.1, 123.4, 119.4, 116.1, 115.2, 114.9, 113.3, 109.9, 56.7, 56.0, 43.8; MS (EI) m/z (%): 348 (M^+ +2, 8), 346 (M^+ , 8), 335 (12), 174 (40), 165 (100), 78 (13), 63 (18), 44 (14).

2-((4-bromophenyl)amino)-2-(naphthalen-1-yl)acetonitrile (4f).

Isolated as yellow solid, (303 mg, 90%), Melting point: 156–158 °C; IR (KBr): ν (cm^{-1}) =

^1H NMR (300 MHz) δ 8.11 – 7.96 (m, 3H), 7.89 (d, J = 7.0, 1H), 7.69 – 7.56 (m, 3H), 7.39 (d, J = 9.0, 2H), 6.95 (t, J = 8.5, 3H), 6.66 (d, J = 9.0, 1H); ^{13}C NMR (101 MHz) δ 145.9, 134.0, 132.2, 130.4, 130.3, 130.2, 129.2, 127.4, 126.9, 126.2, 125.8, 123.8, 119.6, 116.0, 109.8, 47.1; MS (EI) m/z (%): 336 (M^+ , 26), 310 (16), 166 (100), 127 (10), 127 (10). M^+ +2???

2-((4-bromophenyl)amino)-2-(4-methoxyphenyl)acetonitrile (4i).

Isolated as yellow solid, (282 mg, 89%), Melting point: 146–148 °C; IR (KBr): ν (cm^{-1}) =

^1H NMR (300 MHz, CDCl_3) δ 7.54 – 7.45 (m, 2H), 7.40 – 7.32 (m, 2H), 7.02 – 6.92 (m, 2H), 6.70 – 6.61 (m, 2H), 5.32 (d, J = 8.1, 1H), 4.02 (d, J = 8.1, 1H), 3.84 (s, 3H); ^{13}C NMR (75 MHz) δ 160.1, 145.8, 132.0, 129.1, 127.0, 119.9, 116.3, 114.8, 109.7, 55.7, 48.1; MS (EI) m/z (%): 316 (M^+ , 30), 290 (29), 146 (100), 63 (10). M^+ +2???

2-((4-bromophenyl)amino)-2-(naphthalen-2-yl)acetonitrile (4j). **dirty spectra! I do not trust the ¹³C assignment it is too diluted (as it is probably known, please check all the ¹³C signals):**

Isolated as yellow solid, (303 mg, 90%), Melting point: 263–265 °C; IR (KBr): ν (cm⁻¹) =
¹H NMR (300 MHz) δ 8.13 (s, 1H), 8.06 – 7.95 (m, 3H), 7.66 (dd, J = 9.0, 1.8, 1H), 7.62 – 7.55 (m, 2H), 7.38 – 7.32 (m, 2H), 7.03 (d, J = 9.2, 1H), 6.90 – 6.77 (m, 2H), 6.21 (d, J = 9.2, 1H);
¹³C NMR (101 MHz) δ 145.8, 133.3, 133.1, 132.6, 132.1, 129.3, 128.5, 128.1, 127.3 (2c), 126.6, 125.3, 119.6, 116.3, 109.9, 48.8; MS (EI) m/z (%): 336 (M^{+2} , 11), 334 (M^{+} , 11), 327 (14), 155 (100), 127 (51).

2,2'-(1,4-phenylene)bis(2-((4-bromophenyl)amino)acetonitrile) (4q). **Dirty spectra**

Isolated as yellow solid, (446 mg, 90%), Melting point: 194–196 °C; IR (KBr): ν (cm⁻¹) =
¹H NMR (400 MHz) δ 7.67 (s, 4H), 7.37 – 7.32 (m, 4H), 6.96 (dd, J = 9.3, 2.1, 2H), 6.81 – 6.77 (m, 4H), 6.08 (d, J = 8.8, 2H); ¹³C NMR (101 MHz) δ 145.6, 135.9, 132.1, 128.4, 119.5, 116.3, 110.0, 48.3; MS (EI) m/z (%): 495 (M^{+} , 3), 492 (20), 467 (100), 442 (97), 299 (11), 286 (13), 259 (12), 182 (17), 155 (59), 116 (14), 76 (29). **2Br!!!! Check the M peaks distribution!!**

Acknowledgements

We thank Bu-Ali Sina University, the Iran National Science Foundation (INSF, Grant No: 95831207), the National Elites Foundation, the University of Alicante (VIGROB-173), and the Spanish Ministerio de Economía y Competitividad (CTQ2015-66624-P) for financial support to our research groups.

References

1. C. Pérollier and A. B. Sorokin, *Chem. Commun.*, 2002, 1548–1549.

2. B. Meunier and A. Sorokin, *Acc. Chem. Res.*, 1997, **30**, 470–476.
3. A. Sorokin, S. De Suzzoni-Dezard, D. Poullain, J. P. Noel, B. Meunier, *J. Am. Chem. Soc.*, 1996, **118**, 7410–7411.
4. A. Hadasch, A. Sorokin, A. Rabion, L. Fraisse and B. Meunier, *Bull. Soc. Chim. Fr.*, 1997, **134**, 1025–1032.
5. A. Sorokin and B. Meunier, *J. Chem. Soc., Chem. Commun.*, 1994, 1799–1800.
6. A. Sorokin, J.L. Seris and B. Meunier, *Science*, 1995, **268**, 1163–1166.
7. K. Kasuga, K. Mori, T. Sugimori and M. Handa, *Bull. Chem. Soc. Jpn.*, 2000, **73**, 939–940.
8. C. C. Leznoff and A. B. P. Lever, *Phthalocyanines-Properties and Applications*, VCH, New York, 1989–1996, vol. I–IV.
9. H. Zollinger, *Color Chemistry: Synthesis, Properties, and Applications of Organic Dyes and Pigments*, Verlag Helvetica Chimica Acta & Wiley-VCH, Zurich, 3rd edn, 2003.
10. (a) A. L. Thomas, *Phthalocyanine Research and Applications*, CRC Press, Boca Raton, Ann Arbor, Boston, 1990; (b) F. H. Thomas and A. L. Moser, *The Phthalocyanines*, CRC Press, Boca Raton, 1983, vol. 1.
11. (a) S.-I. Ogura, K. Tabata, K. Fukushima, T. Kamachi and I. Okura, *J. Porphyrins Phthalocyanines*, 2006, **10**, 1116-1124; (b) E. A. Lukyanets, *J. Porphyrins Phthalocyanines*, 1999, **3**, 424-432; (c) C. M. Allen, W. M. Sharman and J. E. Van Lier, *J. Porphyrins Phthalocyanines*, 2001, **5**, 161-169; (d) J.-Y. Liu, X.-J. Jiang, W.-P. Fong and D. K. P. Ng, *Org. Biomol. Chem.*, 2008, **6**, 4560-4566.
12. N. B. McKeown, *Phthalocyanine Materials: Synthesis, Structure and Function*, Cambridge University Press, Cambridge, 1998.

13. M. Wyler, US Pat., 2 197 458, 1940.
14. (a) J. W. Steed, D. R. Turner and K. Wallace, *Core Concepts in Supramolecular Chemistry and Nanochemistry*, John Wiley & Sons, Chichester, England, 2007, p. 37; (b) D. K. MacFarland, C. M. Hardin and M. J. Lowe, *J. Chem. Educ.*, 2000, **77**, 1484-1485; (c) H. Z. Gök, H. Kantekin, Y. Gök and G. Herman, *Dyes Pigm.*, 2007, **75**, 606-611; (d) M. N. Kopylovich, V. Y. Kukushkin, M. Haukka, K. V. Luzyanin and A. J. L. Pombeiro, *J. Am. Chem. Soc.*, 2004, **126**, 15040-15041.
15. W. J. Youngblood, *J. Org. Chem.*, 2006, **71**, 3345-3356.
16. (a) H. Tomoda, S. Saito and S. Shiraishi, *Chem. Lett.*, 1983, **3**, 313-316; (b) D. Wöhrle, G. Schnurpfeil and G. Knothe, *Dyes Pigm.*, 1992, **18**, 91-102; (c) C. H. Lee and D. K. P. Ng, *Tetrahedron Lett.*, 2002, **43**, 4211-4214; (d) S. M. S. Chauhan, S. Agarwal and P. Kumari, *Synth. Commun.*, 2007, **37**, 2917-2925; (e) W. Liu, C.-H. Lee, H.-W. Li, C.-K. Lam, J. Wang, T. C. W. Mak and D. K. P. Ng, *Chem. Commun.*, 2002, 628-629; (f) I. Özçeşmeci, A. I. Okur and A. Gül, *Dyes Pigm.*, 2007, **75**, 761-765.
17. T. D. Smith, J. Livorness, H. Taylor, J. R. Pilbrow and G. R. Sinclair, *J. Chem. Soc., Dalton Trans.*, 1983, 1391-1400.
18. R. P. Linstead, E. G. Noble and J. M. Wright, *J. Chem. Soc.*, 1937, 911-921.
19. F. H. Moser and A. L. Thomas, *Phthalocyanines*, A.C.S. Mono-graph 157, Reinhold Publishing Corp., New York, 1963
20. L. J. Boucher, *Coordination Chemistry of Macrocyclic Compounds*, ed. G. A. Melson, Plenum Press, New York, 1979, p. 461.
21. L. F. Lindoy and D. H. Busch, 'Preparative Inorganic Reactions,' ed. W. L. Jolly, Wiley-Interscience, New York, 1971, vol. 6.

22. A. H. Jackson, 'The Porphyrins, I (structure and synthesis. Part A),' ed. D. Dolphin, Academic Press, New York, 1978, p. 365.
23. N. Fukada, *Nippon Kagaku Zasshi*, 1957, 78, 1348 (Chem. Abs, 1959, 53, 12339b).
24. M. Yokote and F. Shibamiya, *Kogyo Kagaku Zudii*, 1958, 61, 994 (Chem. Ah., 1961, 55, 187698).
25. (a) M. Yokote, F. Shibamiya, and S. Tokairin, *Kogyo Kagaku Zasshi*, 1964,67, 166 (Chem. Abs., 1964, 61, 3235f); (b) J. E. Scott, *Histochemie*, 1972, 32, 191; (c) E. G. Gal'pern, E. A. Luk'yanets, and M. G. Gal'pern, *Izo. Akad. Nauk SSSR Ser. Khim.*, 1973,9, 1976; (d) Jawad Alzeer, Phillippe J. C. Roth and Nathan W. Luedtke, *Chem. Commun.*, 2009, 1970–1971
26. M. Yokote, F. Shibamiya, and H. Yokornizao, *Yuki Gosei Kgaku Kyokai Shi*, 1969, 27, 340 (Chem. Abs., 1969,71,38931h).
27. M. Yokote, F. Shibamiya, and N Sakikubo, *Yuki Gosei Kgaku Kyokai Shi*, 1969,27,448 (Chem. Abs., 1969,72,125956p)
28. M. Yokote and F. Shibamiya, *Kogyo Kagaku Zasshi*, 1959, 62, 720 (Chem. Ah., 1962, 57, 9856c)
29. M. G. Gal'pern and E. A. Luk'yanets, *Zh. Obshch. Khim.*, 1969, 39, 2536.
30. (a) A. Strecker, *Ann. Chem. Pharm.*, 1850, 75, 27-45; (b) M. B. Smith and J. March, *March's Advanced Organic Chemistry: Reactions, Mechanisms, and Structure*, 5th edn., Wiley-Interscience, New York p. 1240 (2001).
31. D. Enders and J. P. Shilvock, *Chem. Soc. Rev.*, 2000, 29, 359-373.
32. T. Vilaivan, C. Winotapan, T. Shinada and Y. Ohfuné, *Tetrahedron Lett.*, 2001, 42, 9073-9076.

33. T. Vilaivan, C. Winotapan, V. Banphavichit, T. Shinada and Y. Ohfuné, *J. Org. Chem.*, 2005, **70**, 3464-3471.
34. C.-L. K. Lee, H. Y. Ling and T.- P. Loh, *J. Org. Chem.*, 2004, **69**, 7787-7789.
35. For a discussion of the mechanism, see: B. Molle and P. Bauer, *J. Am. Chem. Soc.*, 1982, **104**, 3481-3487.
36. S. K. De and R. A. Gibbs, *Tetrahedron Lett.*, 2004, **45**, 7407-7408.
37. J. S. Yadav, B. V. Subba Reddy, B. Eeshwaraiah and M. Srinivas, *Tetrahedron* 2004, **60**, 1767-1771.
38. L. Royer, S. K. De and R. A. Gibbs, *Tetrahedron Lett.*, 2005, **46**, 4595-4597.
39. R. Martínez, D. J. Ramón and M. Yus, *Tetrahedron Lett.*, 2005, **46**, 8471-8474.
40. A. S. Paraskar and A. Sudalai, *Tetrahedron Lett.*, 2006, **47**, 5759-5762.
41. B. Das, R. Ramu, B. Ravikanth and K. R. Reddy, *Synthesis* 2006, 1419-1422.
42. (a) S. Harusawa, Y. Hamada and T. Shioiri, *Tetrahedron Lett.*, 1979, **20**, 4663-4666; (b) K. Mai and G. Patil, *Tetrahedron Lett.*, 1984, **25**, 4583-4586; (c) S. Kobayashi and H. Ishitani, *Chem. Rev.*, 1999, **99**, 1069-1094.
43. A. Heydari, P. Fatemi and A.-A. Alizadeh, *Tetrahedron Lett.*, 1998, **39**, 3049-3050.
44. S. K. De and R. A. Gibbs, *J. Mol. Catal. A: Chem.*, 2005, **232**, 123-125.
45. (a) B. A. Horenstein and K. Nakanishi, *J. Am. Chem. Soc.*, 1989, **111**, 6242-6246; (b) J. Mulzer, A. Meier, J. Buschmann and P. Luger, *Synthesis* 1996, 123-132.
46. H. A. Oskooie, M. M. Heravi, K. Bakhtiari, V. Zadsirjan and F. F. Bamoharram, *Synlett* 2006, 1768-1770.
47. B. C. Ranu, S., S. Dey and A. Hajra *Tetrahedron* 2002, **58**, 2529-2532.

48. (a) M. Safaiee, M. A. Zolfigol, F. Afsharnadery and S. Baghery, *RSC Adv.*, 2015, **5**, 102340-102349; (b) M. A. Zolfigol, M. Safaiee and N. Bahrami-Nejad, *New J. Chem.*, 2016, **40**, 5071-5079; (c) M. A. Zolfigol, S. Baghery, A. R. Moosavi-Zare and S. M. Vahdat, *RSC Adv.*, 2015, **5**, 32933-32940; (d) M. A. Zolfigol, S. Baghery, A. R. Moosavi-Zare, S. M. Vahdat, H. Alinezhad and M. Norouzi, *RSC Adv.*, 2015, **5**, 45027-45037.
49. M. G. Dekamin, M. Azimoshan and L. Ramezani, *Green Chem.*, 2013, **15**, 811-820.
50. M. G. Dekamin, Z. Karimi and M. Farahmand, *Catal. Sci. Technol.*, 2012, **2**, 1375-1381.
51. M. G. Dekamin, S. Sagheb-Asl and M. R. Naimi-Jamal, *Tetrahedron Lett.*, 2009, **50**, 4063-4066.
52. M. G. Dekamin, Z. Mokhtari and Z. Karimi, *Sci. Iran. C*, 2011, **18**, 1356-1364.
53. A. R. Hajipour, Y. Ghayeb and N. Sheikhan, *J. Iran. Chem. Soc.*, 2010, **7**, 447-454.
54. A. R. Hajipour and I. Mahboobi Dehbane, *Iran. j. catal.*, 2012, **2**, 147-151.
55. G. K. S. Prakash, T. E. Thomas, I. Bychinskaya, A. G. Prakash, C. Panja, H. Vaghoo and G. A. Olah, *Green Chem.*, 2008, **10**, 1105-1110.
56. (a) G. Hopfengärtner, D. Borgmann, I. Rademacher, G. Wedler, E. Hums and G.W. Spitznagel *J. Electron. Spectrosc. Relat. Phenom.* 1993, **63**, 91-116; (b) B. F. Dzhurinskii, D. Gati, N. P. Sergushin, V. I. Nefedov and Ya. V. Salyn, *Russ. J. Inorg. Chem.*, 1975, **20**, 2307-2314.